Atlantic Arctic Ocean, atmosphere, and sea-ice controls of cold season Greenland coastal air temperatures, 1873-2013

T.J. Ballinger[1], S. Brasher[2], E. Hanna[3], R.J. Hall[3], M. Tedesco[4], and E. Greene[1]

[1]Department of Geography, Texas State University, San Marcos, TX, USA (Email: tballinger@txstate.edu); [2]Department of Geography, University of Delaware, Newark, DE, USA; [3]School of Geography, University of Lincoln, Lincoln, UK; [4]Lamont-Doherty Earth Observatory, Columbia University, Palisades, NY, USA

TEXAS STATE GEOGRAPHY

Abstract

Arctic amplification, the increased warming trend of boreal high latitude surface air temperatures (SAT) relative to lower latitudes, is known to spatiotemporally vary over the observational record with the strongest signal found across cold season months (i.e. October – March). Greenland and the surrounding North Atlantic cryosphere have experienced particularly strong, recent temperature variability and warming in the last 30-40 years, however the interplay of regional oceanic and atmospheric patterns (e.g. Atlantic Multidecadal Oscillation (AMO), North Atlantic Oscillation (NAO), Greenland Blocking (GB)) that contribute to long-term air temperature fluctuations is not well understood. Using a set of Danish Meteorological Institute SAT observations back to 1873, variations in autumn (October – December; OND) and winter (January – March; JFM) Greenland coastal surface air temperatures (SAT) are analyzed and related to long-term, reconstructed marginal sea ice and surface temperature and atmospheric circulation series using a principal component regression approach. Contemporaneous and lagged ocean-atmosphere co-variability with the seasonal air temperature records is assessed through application of multiple statistical models. Preliminary results suggest that temporally coherent (zero-lag) NAO and GB explain 20-40% of the autumn GCT variance, maximized at Narsarsuaq (southern Greenland; ~40%) and diminishing northward at Upernavik (northwest Greenland; ~20%). Smaller amounts of the variance are explained by local Baffin Bay and Labrador Sea ice concentration and AMO, suggesting that regional wind patterns and the background oceanic state modulate cryosphere conditions and feedbacks with SAT beyond the documented coupling within the last half century.

Research Objectives

The primary objectives of this work are to identify the North Atlantic sea ice, ocean, and atmospheric patterns (at lags up to two seasons) that influence Greenland coastal and nearby ablation area ice sheet OND and JFM SAT since the late 19th century.

Study Area

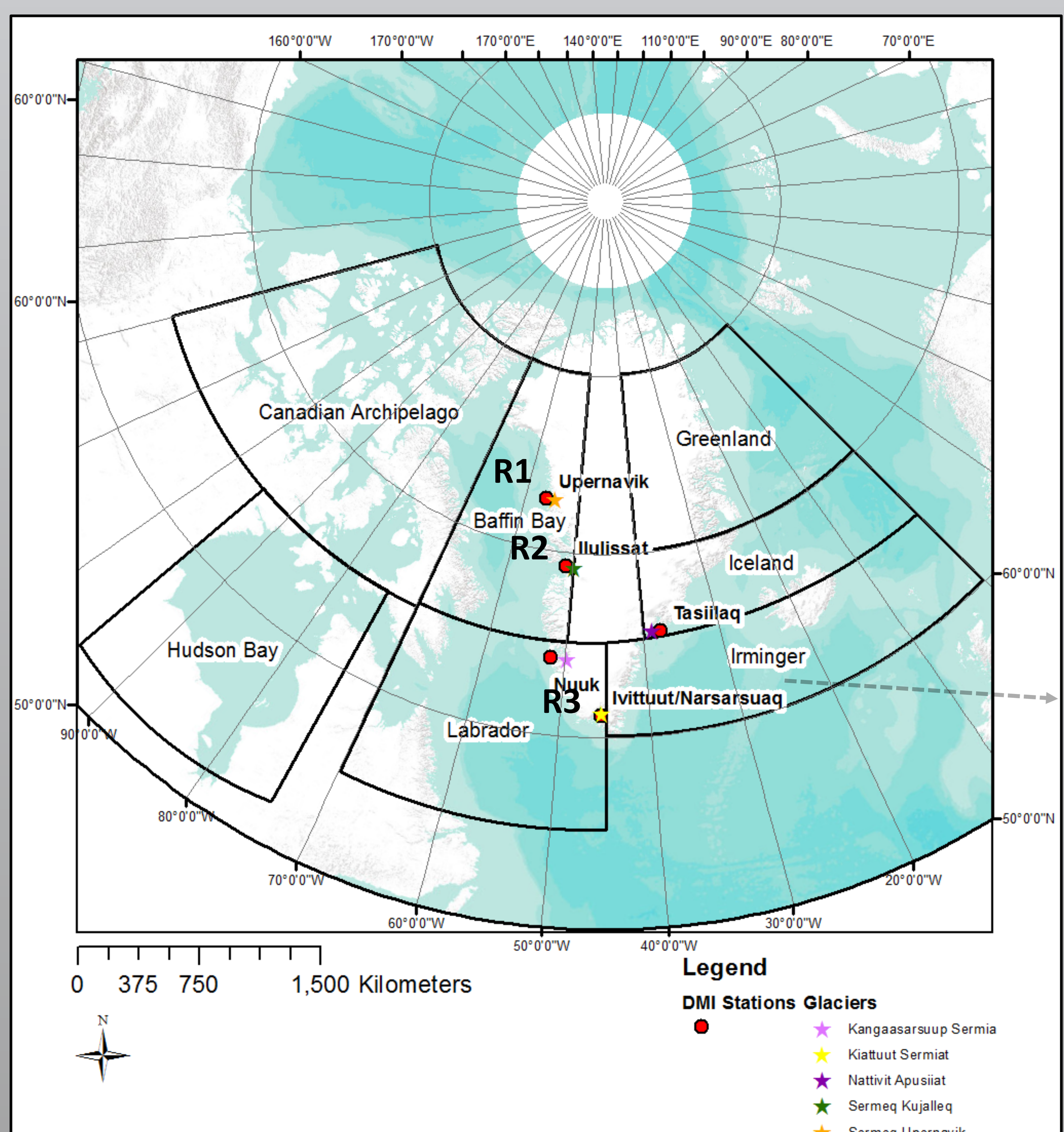

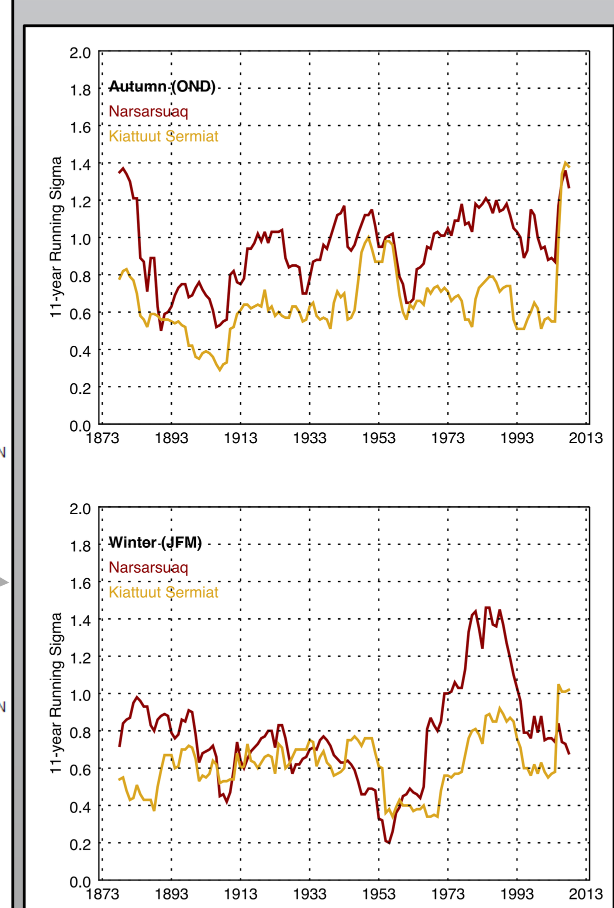

Fig 1. Atlantic Arctic Ocean study area with three emphasized surface air temperature (SAT) regions marked R1, and R2, and R3 shown on the left. The 11-year running standard deviations (sigma) of autumn (OND) and winter (JFM) SAT for Narsarsuaq and Kiattuut Sermiat, 1873-2013, are presented on the right.

Data & Methods

Data (obtained at monthly scale for 1873-2013 period)

- As outlined in **Fig 1**, marginal sea-aggregated Arctic sea ice concentration (SIC) from Walsh et al. (2017), and sea surface temperature (SST) from Hadley Centre Global Sea Ice and Sea Surface Temperature (HadISST) V1.1 (Rayner et al., 2003)
- North Atlantic Oscillation (NAO), East Atlantic (EA) pattern, and Scandinavian (SCA) pattern are resolved from the first three principal components of sea-level pressure over the North Atlantic region (10-80°N, 100°W-40°E; Comas-Bru and Hernández, 2018)
- Greenland Blocking Index (GBI) representing 500 hPa mean geopotential heights over Greenland and surrounding seas (60-80°N, 20-80°W; Hanna et al., 2016)
- Atlantic Multidecadal Oscillation (AMO) of area-weighted, unsmoothed SSTs from 0-70°N over the North Atlantic (Enfield et al., 2001)
- Danish Meteorological Institute (DMI) SAT for west and east coast locales about Greenland (**Fig 1**; Cappelen, 2019)
- Downscaled and topographically-corrected glacier SAT for nearby ice masses to the DMI SATs (see Hanna et al., 2011 and Ballinger et al., 2018 for details of merged datasets)
- Greenlandic naming conventions following Bjork et al. (2015)

Methods

Using a similar framework to Ballinger and Rogers (2014):

- Seasonal (e.g. JFM, AMJ, JAS, OND), normalized indices, by the 1951-2000 base period, are created for all variables and the long-term linear trend is removed
- A rotated principal component (RPC) approach is applied to the seasonal indices; RPCs with eigenvalues >1 are retained and described based on loadings of >0.50
- Lag-0, -1, and -2 season RPC predictability of JFM and OND coastal and ice sheet SAT is assessed by a stepwise multiple linear regression model (significant predictors by the f-test are retained when p≤0.05 and are shown in the description tables and figures)

Results: Autumn

Autumn SAT Analysis: Rotated Principal Component (RPC)	Description (each seasonal index separated by ;)
RPC 1	AMO OND; AMO JAS; AMO AMJ
RPC 3	Labrador SIC OND; Baffin SIC OND; Hudson SIC OND; Canadian SIC OND
RPC 5	Canadian SST JAS; Canadian SST AMJ
RPC 6	NAO OND; GBI OND
RPC 7	Iceland SIC OND; Irminger SIC OND
RPC 8	GBI JAS; NAO JAS
RPC 11	SCA AMJ
RPC 12	Greenland SIC OND

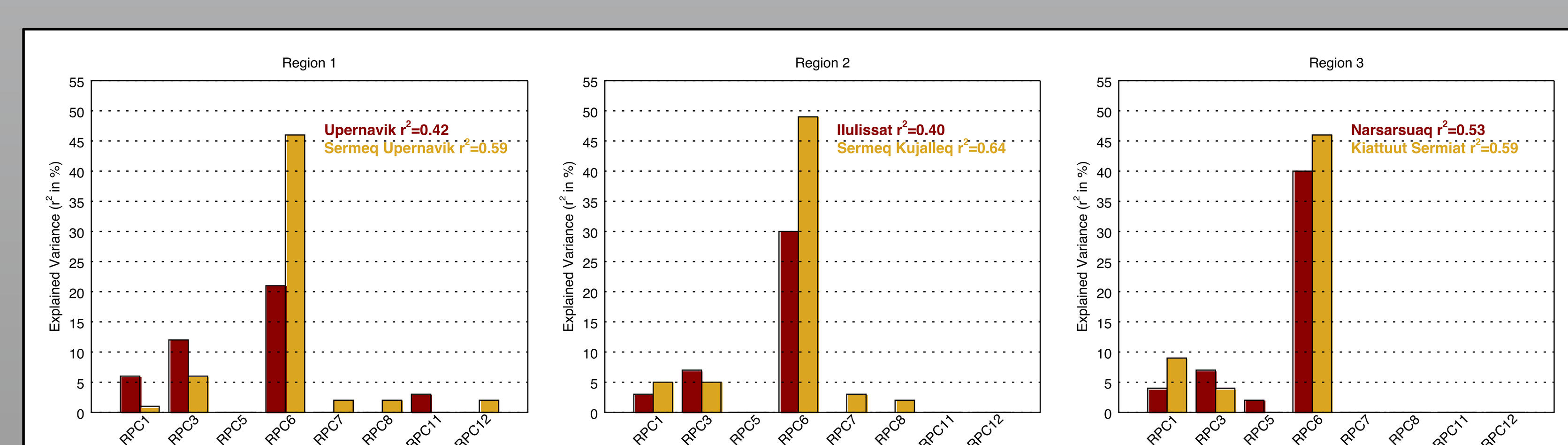

Table 1 and Fig 2. Statistically significant RPC predictors for autumn SATs in regions 1, 2, and 3.

Results: Winter

Winter SAT Analysis: Rotated Principal Component (RPC)	Description (each seasonal index separated by ;)
RPC 1	Iceland SIC JFM; Irminger SIC JFM; Iceland SIC OND; Irminger SIC OND; Greenland SST JAS; Hudson SST JAS
RPC 2	AMO JFM; AMO OND; AMO JAS
RPC 3	Baffin SIC OND; Canadian SIC OND; Hudson SIC OND; Labrador OND SIC
RPC 4	GBI JFM
RPC 7	Baffin SST JAS; Canadian SST JAS
RPC 8	Irminger SST JAS; Iceland SST JAS
RPC 11	Labrador SIC JFM

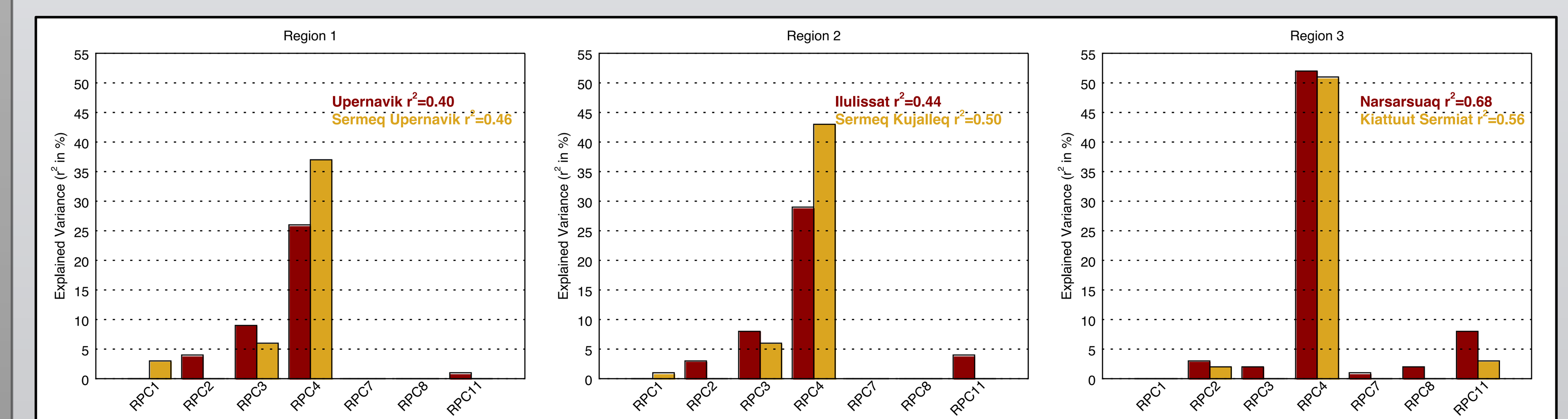

Table 2 and Fig 3. Statistically significant RPC predictors for winter SATs in regions 1, 2, and 3.

Conclusions

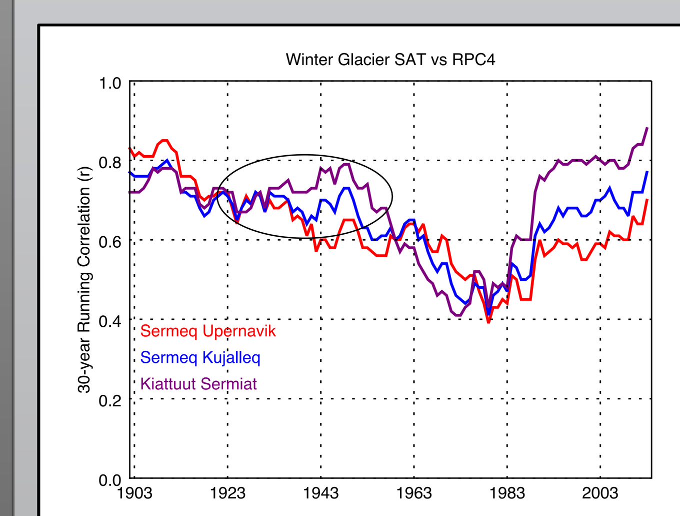

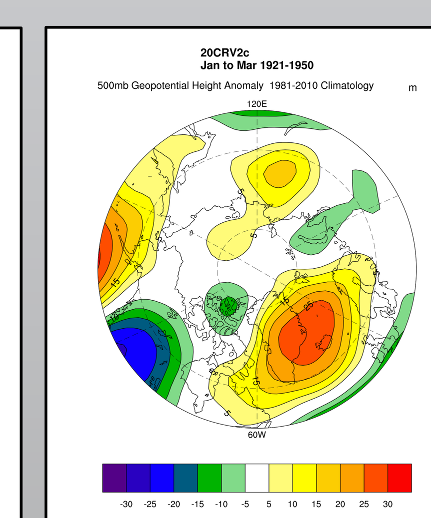

Fig 4. Running correlations of winter glacier SAT versus RPC4 for R1, R2, and R3 (left). A period of persistent, high correlations stretching into the mid-20th century is circled. All coefficients are statistically significant at p≤0.05. The mean JFM 500 hPa geopotential height anomaly for the persistent period is presented on the right.

At least 40% of the long-term coastal and glacier SAT variance, in both autumn and winter, is captured by the RPC indices. Notably, the RPCs tend to predict higher amounts of glacier versus coastal SAT variance, likely due to their decreased variability and consistent "seasonal" air temperatures from processes such as radiational cooling and downsloping katabatic winds.

Future work will explore Nuuk and Tasiilaq and nearby glacier SATs (**Fig 1**) applying similar methods in an attempt to hindcast their 1890s to 2013 temperature variability. The interannual intensity and geographic positioning of Greenland blocks in modulating cold season SATs will also be further explored.

References

Ballinger, T.J., and J.C. Rogers, 2014: Climatic and atmospheric teleconnection indices and western Arctic sea ice variability. Phys. Geog., 35, 459-477, doi:10.1080/02723646.2014.949338.

Ballinger, T.J., E. Hanna, R.J. Hall, J. Miller, M.H. Ribergaard, J.L. Høyer, 2018: Greenland coastal air temperatures linked to Baffin Bay and Greenland Sea ice conditions during autumn through regional blocking patterns. Clim. Dyn., 50, 83-100, doi:10.1007/s00382-017-3583-3.

Bjork, A.A., L.M. Kruse, and P.B. Michaelsen, 2015: Brief communication: Getting Greenland's glaciers right – a new data set of all official Greenlandic glacier names. Cryosphere, 9, 2215-2218, doi:10.5194/tc-9-2215.

Cappelen, J., 2019: Weather observations from Greenland 1958-2018. Observation data with description. DMI Report 19-08. Copenhagen, Denmark.

Comas-Bru, L., and A. Hernandez, 2018: Reconciling North Atlantic climate modes: revised monthly indices for the East Atlantic and the Scandanavian patterns beyond the 20th century. Earth Syst. Sci. Data, 10, 2329-2344, doi:10.5194/essd-10-2329.

Enfield, D.B., A.M. Mestas-Nunez, and P.J. Trimble, 2001: The Atlantic Multidecadal Oscillation and its relationship to rainfall and river flows in the continental U.S., Geophys. Res. Lett., 28: 2077-2080.

Hanna, E., P. Huybrechts, J. Cappelen, K. Steffen, R.C. Bales, E. Burgess, J.R. McConnell, J.P., Steffensen, M. van den Broeke, L. Wake, G. Bigg, M. Griffiths, and D. Savas, 2011: Greenland Ice Sheet surface balance 1870 to 2010 based on Twentieth Century Reanalysis and links with global climate forcing. J. Geophys. Res., 116, doi:10.1029/2011JD016387.

Hanna, E., T.E., Cropper, R.J. Hall, and J. Cappelen, 2016: Greenland Blocking Index 1851-2015: a regional climate change signal. Int. J. Climatol., 36, 4847-4861, doi:10.1002/joc.4673.

Rayner, N.A., D.E. Parker, E.B. Horton, C.K. Folland, L.V. Alexander, D.P. Rowell, E.C. Kent, and A. Kaplan, 2003: Global analyses of sea surface temperature, sea ice, and night marine air temperature since the late nineteenth century. J. Geophys. Res. – Atmos., 108, doi:10.1029/2002JD002670.

Walsh, J.E., F. Fetterer, J.S. Stewart, and W.L. Chapman, 2017: A database for depicting Arctic sea ice variations back to 1850. Geog. Rev., 107, 89-107, doi:10.1111/j.1931-0846.2016.12195.x.